Pigment Epithelium-Derived Factor Suppresses Ischemia-Induced Retinal Neovascularization and VEGF-Induced Migration and Growth

Elia J. Duh,[1] Hoseong S. Yang,[1] Izumi Suzuma,[2] Masaru Miyagi,[3] Elaine Youngman,[1] Keisuke Mori,[1] Miyuki Katai,[2] Lin Yan,[3] Kiyoshi Suzuma,[2] Karen West,[3] Shekar Davarya,[1] Patrick Tong,[1] Peter Gehlbach,[1] Joel Pearlman,[1] John W. Crabb,[3] Lloyd P. Aiello,[2,4,5] Peter A. Campochiaro,[1,6] and Donald J. Zack[1,6,7]

Purpose. To determine the effect of pigment epithelium-derived factor (PEDF) in a mouse model of ischemia-induced retinal neovascularization and on vascular endothelial growth factor (VEGF)–induced migration and growth of cultured microvascular endothelial cells.

Methods. Human recombinant PEDF was expressed in the human embryonic kidney 293 cell line and purified by ammonium sulfate precipitation and cation exchange chromatography. C57BL/6 mice were exposed to 75% oxygen from postnatal day (P)7 to P12 and then returned to room air. Mice received intravitreal injections of 2 μg PEDF in one eye and vehicle in the contralateral eye on P12 and P14. At P17, mice were killed and eyes enucleated for quantitation of retinal neovascularization. The mitogenic and motogeneic effects of VEGF on cultured bovine retinal and adrenal capillary endothelial cells were examined in the presence or absence of PEDF, using cell counts and migration assays.

Results. Two species of human recombinant PEDF, denoted A and B, were purified to apparent homogeneity. PEDF B appeared to comigrate on SDS-PAGE with PEDF from human vitreous samples. Changes in electrophoretic mobility after peptide-*N*-glycosidase F (PNGase F) digestion suggest that both PEDF forms contain N-linked carbohydrate. Analyses of the intact proteins by liquid chromatography–electrospray mass spectrometry (LC-ESMS) revealed the major molecular weight species for PEDF A (47,705 ± 4) and B (46,757 ± 5). LC-ESMS analysis of tryptic peptides indicated that PEDF A and B exhibit differences in glycopeptides containing *N*-acetylneuraminic acid (NeuAc) and *N*-acetylhexosamine (HexNAc). Intravitreal administration of either species of PEDF significantly inhibited retinal neovascularization (83% for PEDF A and 55% for PEDF B; $P = 0.024$ and 0.0026, respectively). PEDF A and B (20 nM) suppressed VEGF-induced retinal microvascular endothelial cell proliferation by 48.8% and 41.4%, respectively, after 5 days ($P < 0.001$) and VEGF-induced migration by 86.5% ± 16.7% and 78.1% ± 22.3%, respectively, after 4 hours ($P = 0.004$ and $P = 0.008$, respectively).

Conclusions. These data indicate that elevated concentrations of PEDF inhibit VEGF-induced retinal endothelial cell growth and migration and retinal neovascularization. These findings suggest that localized administration of PEDF may be an effective approach for the treatment of ischemia-induced retinal neovascular disorders. (*Invest Ophthalmol Vis Sci.* 2002;43: 821–829)

Ocular neovascularization is a visually threatening complication common to a diverse array of ophthalmic conditions, including diabetic retinopathy, retinal vein occlusion, retinopathy of prematurity, and neovascular age-related macular degeneration. VEGF has been demonstrated to play a major role in ocular neovascularization in ischemic retinopathies.[1] It is known to be an endothelial cell mitogen,[2,3] and its expression is induced by hypoxia in tumors[4] and various ocular cell types in culture.[5] VEGF levels have been found to be elevated in the retina and vitreous of patients with ischemic ocular neovascular disorders,[6–8] as well as in animal models of ocular neovascularization.[9–11] In these animal models, inhibition of VEGF[9,10,12,13] or VEGF receptor[14,15] has resulted in a reduction of ocular neovascularization. Based on these observations, the inhibition of VEGF action is a viable approach for the prevention of retinal neovascularization.

Although VEGF plays a major role in retinal neovascularization, it is likely that other molecules, both angiogenic and angiostatic, are involved. Indeed, the angiogenic switch has been postulated to result from an imbalance between angiogenesis stimulators and inhibitors in a given tissue bed.[16] Numerous proangiogenic molecules have been proposed to play a role in retinal neovascularization, including growth hormone and the insulin-like growth factors,[17,18] basic fibroblast growth factor,[19] and hepatocyte growth factor.[20] The role of angiostatic molecules in retinal neovascularization is less well studied. TGF-β has been proposed as an inhibitor of retinal neovascularization.[21] Several systemic inhibitors of angiogenesis have been characterized, including angiostatin,[22] endostatin,[23] antithrombin III,[24] thrombospondin,[25] and platelet factor-4.[26] However, the role of these molecules in retinal neovascularization is unclear, and their potential clinical usefulness as mod-

From the Departments of [1]Ophthalmology, [6]Neuroscience, and [7]Molecular Biology and Genetics, Johns Hopkins University School of Medicine, Baltimore, Maryland; the [2]Research Division and [4]Beetham Eye Institute, Joslin Diabetes Center, Boston, Massachusetts; the [5]Department of Ophthalmology, Harvard Medical School, Boston, Massachusetts; and [3]Cole Eye Institute, Cleveland Clinic Foundation, Cleveland, Ohio.

Supported in part by Grant JDF 4-1999-408 from the Juvenile Diabetes Foundation; the Foundation Fighting Blindness grants to the Wilmer AMD Center and Cole Eye Institute Research Center; National Eye Institute Grants EY00398 and EY06603 and Core Grant EY01765; unrestricted funds from Research to Prevent Blindness (RPB); the Ruth and Milton Steinbach Foundation; the Macula Vision Foundation; and funds from Michael Panitch; Mrs. Harry J. Duffey; and the Cleveland Clinic Foundation. EJD is a recipient of an RPB Career Development Award. LPA is an RPB Dolly Green Scholar. DJZ is the Guerrieri Professor of Genetic Engineering and Molecular Ophthalmology.

Submitted for publication March 13, 2001; revised October 23, 2001; accepted November 1, 2001.

Commercial relationships policy: N.

The publication costs of this article were defrayed in part by page charge payment. This article must therefore be marked "*advertisement*" in accordance with 18 U.S.C. §1734 solely to indicate this fact.

Corresponding author: Donald J. Zack, The Johns Hopkins University School of Medicine, Maumenee 809, 600 N. Wolfe Street, Baltimore, MD 21287; dzack@jhmi.edu.

ulators of neovascularization in vivo has yet to be fully explored.

Recently, pigment epithelium-derived factor (PEDF) has emerged as a potentially important endogenous inhibitor of ocular neovascularization. It is a member of the serine protease inhibitor (serpin) family, although it does not have protease inhibitory activity.[27–29] It was initially purified from the conditioned media of human RPE cells and found to induce neuronal differentiation of cultured Y79 retinoblastoma cells.[30] PEDF also has neuroprotective activity[31–36] and has been demonstrated to protect photoreceptors from degeneration.[37–39] It is interesting to note that PEDF has been found to inhibit neovascularization in a corneal pocket assay and inhibits migration of cultured adrenal capillary endothelial cells.[40] In addition, PEDF has been found in the vitreous and cornea,[40,41] and it has been found to be downregulated by hypoxia in cultured cells.[40] Its presence in the vitreous and its antiangiogenic activity suggest a possible role for PEDF in the regulation of retinal neovascularization. Indeed, a recent study has demonstrated that systemic administration of PEDF significantly inhibits retinal neovascularization in a mouse model.[42]

Because systemic administration of antiangiogenic therapies has a potential for adverse systemic effects,[43] the effects of local administration of PEDF is of interest for the possible treatment of retinal neovascularization. In this study, we explored the anti-angiogenic potential of PEDF on retinal neovascularization in a mouse model, using intravitreal administration. We also analyzed the effect of PEDF on VEGF-induced growth and migration of cultured retinal microvascular endothelial cells and partially characterized the structural differences between two different forms of PEDF.

METHODS

Cloning of Human PEDF

An anti-PEDF peptide antibody was generated by immunizing rabbits with a keyhole limpet hemocyanin-coupled peptide corresponding to amino acids 327-343 of human PEDF, as described.[40] An N-terminal cysteine was added to facilitate the coupling reaction. Antisera were affinity purified against the peptide and renatured.

A human PEDF expressed-sequence tag (EST) containing the entire open reading frame for PEDF (Image clone 235156) was obtained from Research Genetics (Huntsville, AL). The entire EST was cloned into the vector pRK KS, downstream of the cytomegalovirus (CMV) promoter. The resultant construct was cotransfected with pRSV-neomycin into human embryonic kidney (HEK)293 carcinoma cells (Life Technologies, Rockville, MD). Stable transfectants were selected using geneticin (G418; Life Technologies) and screened for PEDF production, using the rabbit anti-PEDF peptide antibody described earlier. The transfection with the strongest expression (C7) was used for subsequent expression and purification of PEDF protein. pRK KS[44] and pRSV-neomycin[45] were generous gifts from Jeremy Nathans (Johns Hopkins University School of Medicine, Baltimore, MD).

Expression and Purification of PEDF

The C7 stable transfectant was grown to confluence and subjected to 24-hour cycles of DMEM with 1× nonessential amino acids, 1× penicillin-streptomycin, and 200 μg/mL geneticin, alternating with the same medium, supplemented with 10% fetal calf serum. Conditioned serum-free medium was collected and ammonium sulfate precipitation (80%) performed to recover protein. The precipitate was resuspended in 20 mM sodium phosphate (pH 7.4), containing 150 mM NaCl. Purification of PEDF was performed using a method similar to Stratikos et al.,[46] with slight modification. This preparation was desalted by gel filtration chromatography (Amersham Pharmacia Biotech, Piscataway, NJ) and then fractionated by cation exchange FPLC chromatography (Amersham Pharmacia Biotech), at pH 6.2, using a 50 to 500 mM NaCl gradient. Two PEDF species were recovered from FPLC that were electrophoretically homogeneous and migrated in the 46- to 49-kDa range. The yields of PEDF B and A were approximately 5 and 1.5 mg/L of media, respectively. Western blot analysis demonstrated positive reactivity with the rabbit anti-PEDF peptide antibody described earlier. PEDF concentrations were determined by a protein assay (Bio-Rad, Hercules, CA).

Patient Vitreous Sample Collection

All research involving human subjects adhered to the tenets of the Declaration of Helsinki. Institutional review and approval was obtained from the Johns Hopkins Joint Committee on Clinical Investigation. Clinical data were obtained from the surgeon before or at the time of surgery.

At the beginning of vitrectomy, undiluted vitreous samples were collected in sterile tubes, placed immediately on ice, clarified by centrifugation, and rapidly frozen at −80°C until analysis by SDS-PAGE and Western blot analysis. The specimens were classified and labeled in anonymous fashion.

Endoglycosidase Digestions

PEDF A and B (0.01 μg each) were treated with 10 U of peptide-*N*-glycosidase F (PNGase F; Prozyme, San Leandro, CA) for 1 hour at 37°C, according to manufacturer's instructions.

Electrophoresis and Western Blot Analysis

Protein preparations and vitreous samples were resolved by 10% SDS-PAGE according to Laemmli.[47] After electrophoresis, proteins were visualized by zinc staining (Bio-Rad). The gel was subsequently transferred to a nitrocellulose membrane (Hybond ECL; Amersham Pharmacia Biotech) for Western blot analysis using as primary antibody either a rabbit anti-PEDF peptide antibody or a mouse monoclonal anti-PEDF antibody (Chemicon, Temecula, CA). A donkey anti-rabbit IgG antibody and a sheep anti-mouse IgG antibody (Amersham Pharmacia Biotech) were used as the secondary antibody. Immunoreactivity was detected by chemiluminescence (Amersham Pharmacia Biotech).

Amino Acid Analysis and Edman Degradation

Phenylthiocarbamyl amino acid analysis was performed using an automated analysis system (model 420H/130/920; Applied Biosystems, Foster City, CA).[48] N-terminal analysis by Edman degradation of PEDF A (50 pmol) and B (50 pmol) quantified by amino acid analysis was performed in the Molecular Biotechnology Core Laboratory, Lerner Research Institute, Cleveland Clinic Foundation and in the Protein Sequencing Core Facility at Johns Hopkins University, using a protein sequencer (Procise Model 492; Applied Biosystems).

Mass Spectrometry

Electrospray mass spectrometry (ESMS) and liquid chromatography ESMS (LC-ESMS) were performed with a triple quadrupole mass spectrometer (Sciex API 3000; PE-Applied Biosystems).[49,50] Nitrogen was used as the nebulizer (at 40 psi) and curtain gas and was supplied by a nitrogen generator (Whatman model 75-72; Parker Hannifin Corp., Cleveland, OH). For LC-ESMS of intact proteins, a scan range of mass-to-charge ratio (m/z) 700 to 1800 was used with 0.2-atomic-mass-unit (amu) steps, a scan time of 7.5 seconds, and an orifice potential of 80 and 5000-V ion spray. Reverse phase (RP)-HPLC of intact proteins was performed at a flow rate of 5 μL/min on a 5-μm C18 capillary column (0.3 × 150 mm, LC Packing; Vydac, Hesperia, CA) using a commercial HPLC system (model 140D; PE-Applied Biosystems) and aqueous acetonitrile-trifluoroacetic acid solvents with 100% of eluant going to the mass spectrometer.

For peptide characterization, purified PEDF A and B (10 μg each) were reduced with dithiothreitol and digested with trypsin (Promega) in 2 M urea and 100 mM ammonium bicarbonate (0.2 μg trypsin, overnight at 37°C). Tryptic peptide mapping was performed with a

matrix-assisted laser desorption-ionization–time-of-flight (MALDI-TOF) mass spectrometer (Voyager DE Pro; PE-Applied Biosystems) with α-cyano-4-hydroxycinnamic acid as the matrix, using methods described elsewhere.[51] Tryptic peptides were also analyzed by LC tandem mass spectrometry (LC-MS/MS) using a mass spectrometer equipped with a liquid chromatography system (CapLC; Quadrupole-Time Of Flight [QTof]; Micromass, Manchester, UK). For LC-MS/MS, peptide digests were trapped and desalted on a precolumn (0.3 × 5 mm, 5 μm C18, LC Packing) with 0.1% formic acid in 2% acetonitrile as loading solvent then eluted onto a capillary column (0.075 × 50 mm, 5 μm C18, 15 μm tip internal diameter, PicoFrit; New Objective, Inc., Woburn, MA). The chromatography was performed at 250 nL/min aqueous acetonitrile-formic acid solvents with 100% of eluant going to the mass spectrometer. Nanoelectrospray ionization was performed with a z-spray source and 3 kV applied to the column. Cone voltage was 35 V and argon was used as collision gas. Data-dependent survey scans selected the three most intense precursor ions on each MS scan for MS/MS data acquisition. MS/MS spectra were collected over the range m/z 50 to 2000.

For glycopeptide characterization, PEDF A and B tryptic digests were analyzed by LC-ESMS, using selective ion monitoring with the triple-quadrupole mass spectrometer (Sciex API 3000; PE-Applied Biosystems), the RP-HPLC system described earlier for intact protein analyses, and previously described methods.[50] Glycopeptides were selectively detected based on diagnostic sugar oxonium ions HexNAc (produced by GalNAc or GlcNAc, m/z 204) and NeuAc (*N*-acetylneuraminic acid, m/z 292). Carbohydrate marker ions at m/z 204 and 292 (dwell time, 200 ms each) were monitored in positive ion mode at high orifice potential (180 V), whereas full scans at m/z 300 to 2300 (0.2-amu steps, scan time 3.5 seconds) were acquired at a lower orifice potential (70 V). In this way, both intact parent ions and abundant marker ions were observed in the same m/z scan.

Mouse Model of Oxygen-Induced Ischemic Retinopathy

Retinal neovascularization was produced in C57BL/6 mice as described.[52] At postnatal day (P)7, mice and their mothers were placed in an incubator and exposed to an atmosphere of 75% ± 1% oxygen for 5 days, at a temperature of 23 ± 2°C. Oxygen was continuously monitored with an oxygen controller (PROOX model 110; Reming Bioinstruments Co., Redfield, NY). Mice were returned to room air at P12.

At P12 and P14, mice received an intravitreal injection of 1 μL PEDF (2 μg/μL) in one eye and vehicle (50 mM sodium phosphate [pH 6.2], 250 mM sodium chloride) in the contralateral eye. Intravitreal injections were performed with a pump microinjection apparatus (Harvard Apparatus, South Natick, MA) and pulled-glass micropipets. Each micropipet was calibrated to deliver a 1-μL volume on depression of a foot switch. The mice were anesthetized, and under a dissecting microscope, the sharpened tip of the micropipet was passed through the sclera just posterior to the limbus into the vitreous cavity and the foot switch depressed. At P17, the mice were killed, and eyes were rapidly removed and frozen in optimum cutting temperature (OCT) embedding compound (Miles Diagnostics, Elkhart, IN) to measure the amount of retinal neovascularization in each eye. The study protocol adhered to the ARVO Statement for the Use of Animals in Ophthalmic and Vision Research.

Quantitation of Retinal Neovascularization

Quantitation of retinal neovascularization was performed as previously described.[15] Ten-micrometer frozen sections of eyes from injected mice were histochemically stained with biotinylated *Griffonia simplicifolia* lectin B4 (GSA; Vector Laboratories, Burlingame, CA), which selectively binds to endothelial cells. Slides were incubated in methanol/H_2O_2 for 10 minutes at 4°C, washed with 0.05 M Tris-buffered saline, pH 7.6 (TBS), and incubated for 30 minutes in 10% normal porcine serum. Slides were incubated for 2 hours at room temperature with biotinylated GSA and after rinsing with 0.05 M TBS, they were incubated with avidin coupled to alkaline phosphatase (Vector Laboratories) for 45 minutes at room temperature. After being washed for 10 minutes with 0.05 M TBS, slides were incubated with a red stain (Histomark Red; Kirkegaard and Perry, Gaithersburg, MD) to give a red reaction product that is distinguishable from melanin.

To perform quantitative assessments, 10-μm serial sections were cut through half of each eye, and sections roughly 100 μm apart were stained with GSA, providing 13 sections per eye for analysis. GSA-stained sections were examined with a microscope (Axioskop; Carl Zeiss, Thornwood, NY) and images were digitized using a 3 color charge-coupled device (CCD) video camera and a frame grabber. A computer and image-analysis software (Image-Pro Plus software; Media Cybernetics, Silver Spring, MD) was used to delineate GSA-stained cells on the surface of the retina, and their area was measured. The mean of the 13 measurements from each eye was used as a single experimental value. All measurements were performed in a masked fashion.

Blue Dye Staining

Ten-micometer frozen sections were fixed with 4% paraformaldehyde for 30 minutes and washed with 0.05 M Tris buffered saline (TBS). Specimens were stained with blue dye (Contrast Blue; Kirkegaard and Perry) according to the manufacturer's instructions. Sections were then dehydrated and mounted in acrylic resin medium (Cytoseal XYL; Richard-Allan Scientific, Kalamazoo, MI).

Cell Culture

Primary cultures of bovine retinal microvascular endothelial cells (BRECs) were isolated by homogenization and a series of filtration steps, as described previously.[53] BRECs were subsequently cultured in endothelial basal medium (Clonetics, San Diego, CA) with 10% plasma-derived horse serum, 50 mg/L heparin, and 50 μg/mL endothelial cell growth factor (ECGF, Roche Molecular Biosciences, Indianapolis, IN) in fibronectin-coated dishes. The cells were cultured in 5% CO_2 at 37°C, and media were changed every 3 days. Endothelial cell homogeneity was confirmed by immunoreactivity with anti-factor VIII antibody. Cells were plated at a density of 2×10^4 cells/cm^2 and passaged when confluent. The media were changed every 3 days, and BRECs from passages 4 to 10 were used for experiments. Bovine adrenal gland capillary microvascular endothelial cells (bAGCECs; Clonetics) were cultured in endothelial basal medium with 5% fetal bovine serum, 10 μg/mL human recombinant epidermal growth factor, 1.0 mg/mL hydrocortisone, 50 mg/mL gentamicin, and 3 mg/mL bovine brain extract. Cells were plated at a density of 1×10^4 cells/cm^2 in culture flasks and cultured in 5% CO_2 at 37°C. The media were changed every 2 days; only cells from passages 1 to 3 were used for experiments.

Growth Assay

BRECs were plated sparsely (~5×10^3 cells/well) into 12-well plates (Costar, Cambridge, MA) overnight in DMEM containing 10% calf serum (Gibco, Grand Island, NY). The next day, cells were exposed to PEDF at the concentration indicated with or without VEGF (25 ng/mL). After incubation at 37°C for 4 days, the cells were lysed in 0.1% SDS, and DNA content was measured using Hoechst 33258 dye and a fluorometer (model TKO-100; Hoefer Scientific Instruments, San Francisco, CA).

Migration Assay

Migration was performed using modified Boyden chambers containing polycarbonate membrane (Transwell, 8.0 μm pore size; Costar) with a slight modification from the previously described method.[54] BRECs were seeded at 1×10^4 cells/well (1×10^5 cells/well for bAGCECs) on plates (Transwell; Costar) coated with collagen (10 μg/mL) overnight in DMEM containing 2% calf serum. The next day, media (DMEM/2% calf serum) containing PEDF with or without VEGF (25 ng/mL) were added to the lower chamber. After incubation at 37°C for 4 hours, the

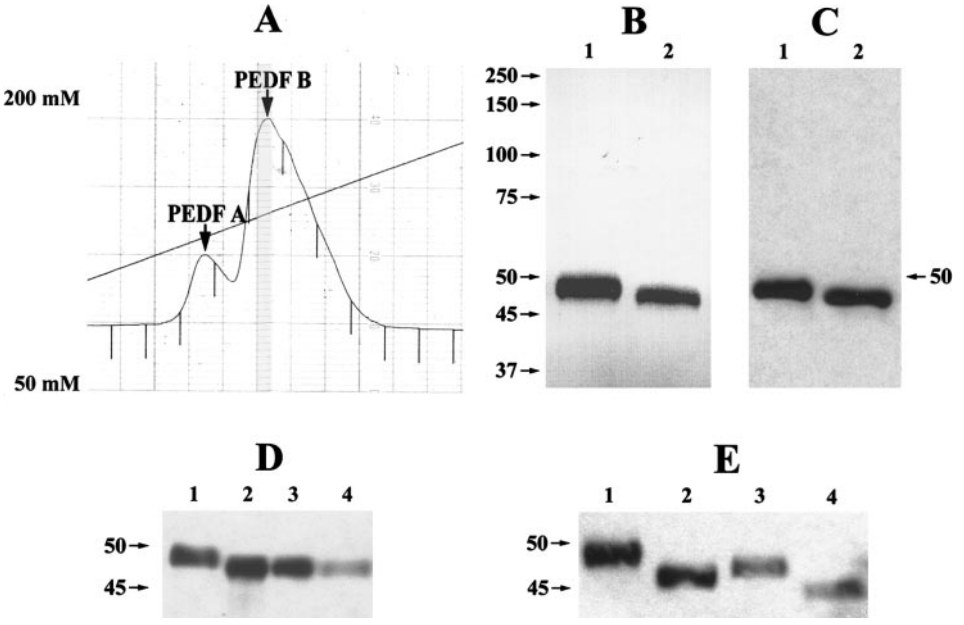

FIGURE 1. SDS-PAGE characterization of purified PEDF. PEDF protein was purified from the HEK293 cell line stably transfected with a plasmid encoding human *PEDF* downstream of the CMV promoter. (**A**) Cation exchange chromatography yielded two peaks, denoted PEDF A and B, in a molar ratio of approximately 1:3. The *diagonal line* indicates the NaCl concentration (range shown on *y*-axis) at which forms A and B eluted. (**B**) Each species (0.5–1.0 μg) was run individually on 10% SDS-PAGE. After electrophoresis, proteins were visualized by zinc staining. *Lane 1*: PEDF A; *lane 2*: PEDF B. (**C**) The gel was subsequently transferred to a nylon membrane for Western blot analysis using a rabbit anti-PEDF peptide antibody. *Lane 1*: PEDF A; *lane 2*: PEDF B. (**D**) In a separate experiment, PEDF A (*lane 1*) and B (*lane 4*) were resolved by SDS-PAGE along with two human vitreous samples (*lanes 2* and *3*), followed by Western blot analysis, with a mouse monoclonal anti-PEDF antibody. (**E**) Western blot analysis (with mouse monoclonal anti-PEDF antibody) of PEDF A, with (*lane 2*) or without (*lane 1*) PNGase F treatment and PEDF B, with (*lane 4*) or without (*lane 3*) PNGase F treatment. *Arrows*: molecular weight markers in kilodaltons.

upper surface of the filter was scraped with a cotton-tipped stick to remove nonmigrated cells, and membranes were fixed with 70% ethanol. Migrated cells were counted using automated computer software (Phase 3 imaging system; Media Cybernetics) under an inverted microscope (AX70TRF; Olympus, Tokyo, Japan) using a ×40 objective, after nuclear staining with green nucleic acid stain (Molecular Probes, Leiden, The Netherlands).

RESULTS

Structural Characterization of Expressed PEDF Protein

HEK293 carcinoma cells were stably transfected with a plasmid containing the open reading frame for human PEDF under the direction of the CMV promoter. PEDF protein was purified from this cell line, by using ammonium sulfate fractionation and cation exchange chromatography. Two chromatography peaks were obtained, denoted A and B, that contained electrophoretically homogeneous components in the 46- to 49-kDa range (Fig. 1B). The chromatographic elution profile suggested that the ratio of PEDF A to PEDF B was approximately 1:3 (Fig. 1A). Furthermore, both showed positive reactivity with a rabbit anti-PEDF peptide antibody on Western blot analysis (Fig. 1C).

In a separate experiment, the two species of PEDF were resolved by SDS-PAGE in conjunction with two human vitreous samples. Western blot analysis, using a mouse monoclonal antibody to human PEDF (Chemicon), disclosed a single band in the human vitreous samples that comigrated with PEDF B (Fig. 1D).

Edman degradation in two independent laboratories with up to 50 pmol of each protein revealed blocked N-terminal sequences for both forms. No contaminating sequences were detected during Edman analysis. Amino acid analysis demonstrated similar amino acid compositions for each form that were within the experimental error of the sequence-determined composition (Table 1). Peptide mapping by MALDI-TOF MS and LC-MS/MS identified peptides accounting for approximately 55% of the protein sequence from each form and support the structural integrity and similarity of the recombinant preparations.

Consistent with the results reported with PEDF expressed in infant hamster kidney cells,[46] both PEDF A and B were found to be glycosylated, as indicated by an increase in SDS-PAGE mobility after PNGase F treatment (Fig. 1E). Analyses of the intact proteins by LC-ESMS revealed the major molecular weight species for PEDF A (47,705 ± 4) and B (46,757 ± 5). For both intact PEDF forms, minor molecular species were also apparent by LC-ESMS analyses that differed by mass increments

TABLE 1. Amino Acid Analysis of Human PEDF

Amino Acid	Symbol	Sequence Composition*	PEDF A	PEDF B
Asp/Asn	D/N	36	38.7	36.5
Glu/Glu	E/Q	40	34.8	38.8
Ser	S	36	35.1	43.1
Gly	G	21	20.8	21.4
His	H	7	5.2	6.3
Arg	R	18	14.4	16.9
Thr	T	28	24.0	28.8
Ala	A	23	22.2	23.9
Pro	P	29	31.6	32.0
Tyr	Y	10	10.4	10.3
Val	V	24	25.0	24.0
Met	M	6	5.9	4.3
Ile	I	21	21.1	19.2
Leu	L	51	54.5	52.4
Phe	F	18	18.4	18.1
Lys	K	27	27.7	27.4
Amount analyzed (μg)			0.6	0.9
Average compositional error (%)			7	7

* Based on PEDF precursor residues 20 to 418.

Compositions were determined by phenylthiocarbamyl amino acid analysis of the purified proteins.[48] Data (in residues per molecule) are uncorrected for partial destruction, incomplete hydrolysis, or contamination from solvents. Cys and Trp were not determined.

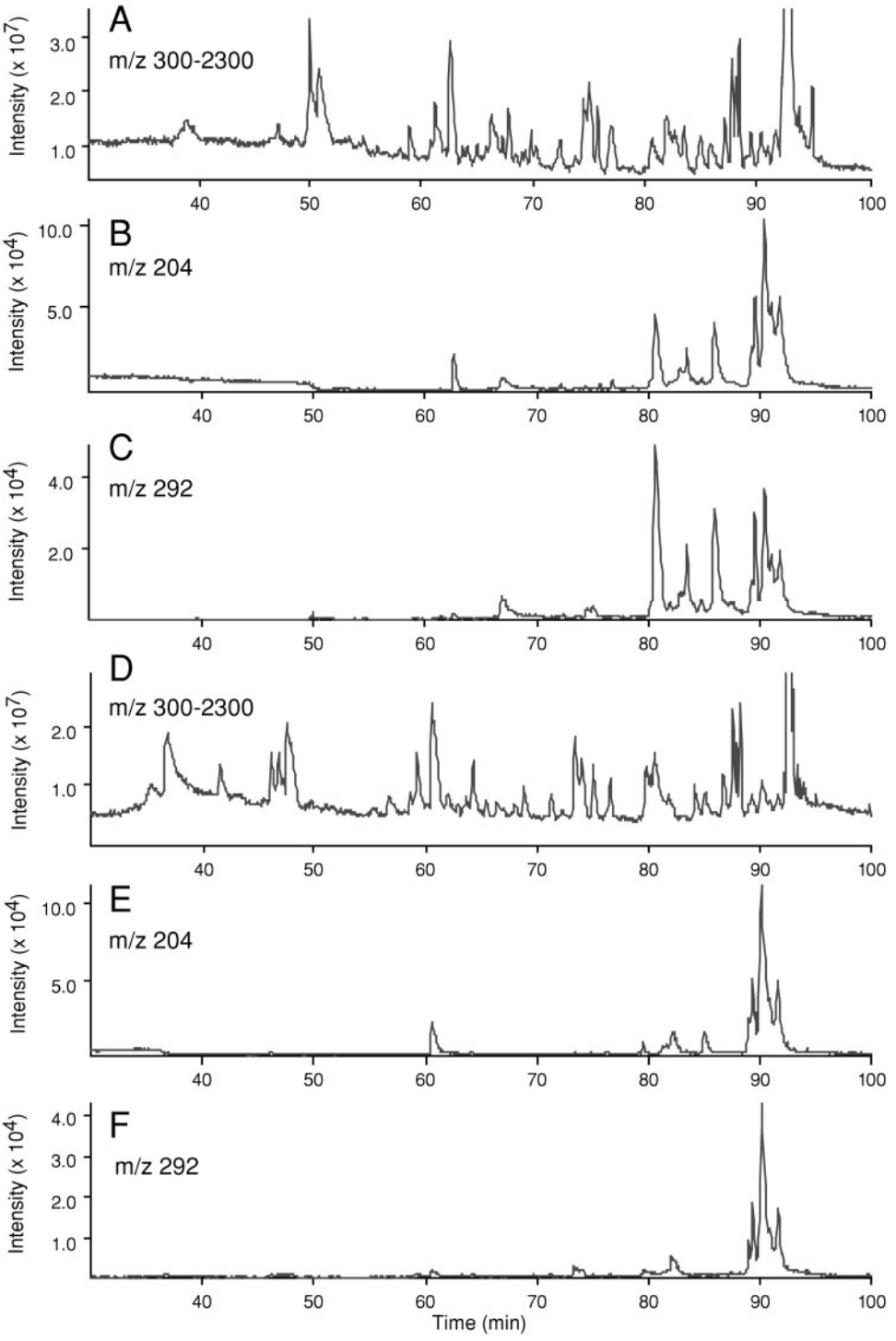

FIGURE 2. LC-ESMS of tryptic digests of human recombinant PEDF. Purified PEDF forms A and B were digested with trypsin and LC-ESMS performed with a triple-quadrupole mass spectrometer, using stepped collision-energy scanning. (**A**) LC-ESMS of PEDF A tryptic digest (~40 pmol). Total ion current (TIC) for the full scan m/z 300 to 2300 is shown. Selective ion monitoring for carbohydrate marker ions (**B**) m/z 204 and (**C**) m/z 292 for (**A**). (**D**) LC-ESMS of PEDF B tryptic digest (~40 pmol). TIC for the full scan m/z 300 to 2300 is shown. Selective ion monitoring for carbohydrate marker ions (**E**) m/z 204 and (**F**) m/z 292 for (**D**).

that approximated the in-chain chemical average mass of oligosaccharide residues (e.g., Hex, 162; HexNAc, 203; and NeuAc, 291). To compare further the glycosylation associated with PEDF A and B, tryptic digests of the each protein were analyzed by LC-ESMS using stepped collision-energy scanning to produce carbohydrate-specific marker ions. Overall peptide similarity between the glycoforms is apparent in the total-ion-current full-scan profiles (Figs. 2A, 2D). Apparent differences in tryptic glycopeptides between the two PEDF forms were observed for HexNAc- (Figs. 2B, 2E) and NeuAc-containing glycopeptides (Figs. 2C, 2F).

PEDF's Effect on Retinal Neovascularization

The effect of PEDF protein on retinal neovascularization in vivo was evaluated using a mouse model of ischemic retinopathy.[52] In this model, C57BL/6 mice are exposed to 75% oxygen from P7 to P12, which results in extensive retinal capillary obliteration. On return of these mice to room air on P12, the inner retina becomes relatively hypoxic, leading to the formation of retinal neovascularization in 100% of animals by P17.[52]

Intravitreal injection of 2 μg PEDF protein in one eye and vehicle in the contralateral eye was performed at P12 and P14.

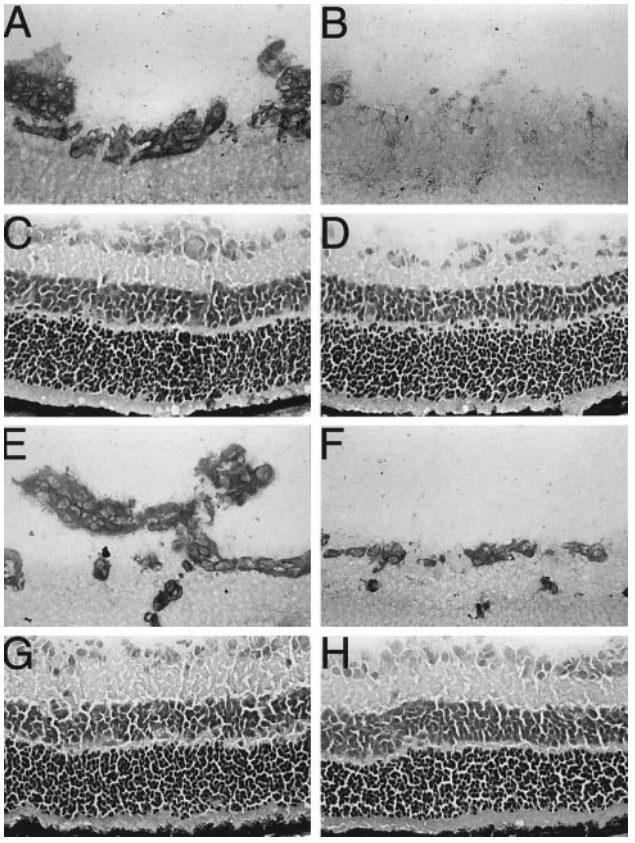

FIGURE 3. Inhibition of ischemia-induced retinal neovascularization in vivo by intravitreous administration of PEDF protein. C57BL/6 mice were exposed to a retinal neovascularization–inducing protocol. Mice received intravitreal injection of 2 μg PEDF in one eye and vehicle in the contralateral eye at P12 and P14. At P17, mice were killed and eyes enucleated for quantitation of retinal neovascularization. Serial frozen sections were stained with GSA, which selectively stains vascular cells. Eyes injected with (**B**) PEDF A or (**F**) B exhibited markedly reduced neovascularization on the retinal surface, compared with contralateral control eyes injected with vehicle (**A**, **E**). Adjacent sections were stained with blue dye. Retinal sections of eyes injected with PEDF A (**D**) and B (**H**) were similar to sections of contralateral eyes injected with vehicle (**C**, **G**).

In eyes injected with vehicle (Figs. 3A, 3E), there was more extensive retinal neovascularization than in eyes injected with either PEDF A (Fig. 3B) or B (Fig. 3F). Quantitation of surface retinal neovascularization is depicted in Figure 4. In 100% of the mice studied ($N = 13$), injection of either PEDF A (Fig. 4A) or B (Fig. 4B) markedly reduced retinal neovascularization, compared with control injection in the contralateral eye ($P = 0.024$ and $P = 0.0026$, respectively, by paired t-test). The PEDF-induced inhibition of retinal neovascularization in individual mice ranged from 59% to 99% with PEDF A and from 41% to 98% with PEDF B. On average, PEDF A reduced retinal neovascularization by 83% and PEDF B by 55% across all eyes tested. It should be noted that more neovascularization was observed overall in the control eyes of the animals injected with PEDF B, compared with those injected with PEDF A, consistent with litter-to-litter variability.

Blue Dye Staining of Retinal Sections

To study the possible toxicity of PEDF protein injection, 10-μm sections adjacent to those sections used to quantitate retinal neovascularization were stained with blue dye (Contrast Blue; Kirkegaard and Perry) and analyzed. Sections obtained from eyes injected with PEDF A or B (Figs. 3D, 3H, respectively) did not show significant difference from sections obtained from contralateral eyes injected with vehicle alone (Figs. 3C, 3G).

PEDF's Effect on VEGF-Induced Retinal Endothelial Cell Migration

VEGF induces retinal endothelial cell migration, which is thought to play an important role in the retinal neovascular response. To determine whether PEDF would affect VEGF-induced migration of BRECs in culture, cells were treated with various concentrations of PEDF or control, and migration was measured after 4 hours. As shown in Figure 5, neither PEDF A nor B had an effect on basal endothelial cell migration at a concentration of 2 nM. VEGF (25 ng/mL) increased endothelial cell migration by 132% ± 38.7% ($P = 0.007$). Addition of 2 nM PEDF A or B suppressed VEGF-induced migration by 60.9% ± 25.1% ($P = 0.034$) and 48.8% ± 18.1% ($P = 0.049$), respectively. Addition of 20 nmol/L PEDF A or B resulted in only slightly more suppression of migration, with inhibition of 86.5% ± 16.7% ($P = 0.004$) and 78.1% ± 22.3% ($P = 0.008$), respectively. VEGF induced migration in the presence of either 2 or 20 nM PEDF was not statistically different from control cells not exposed to VEGF.

Similar results were observed with VEGF-induced migration of bAGCECs, in which 25 ng/mL VEGF increased migration 168% ± 7% ($P < 0.001$) after 4 hours. Addition of 0.02 nM PEDF decreased VEGF-induced migration by 38%, but this was not statistically significant. In contrast, 2.0 nM PEDF A and B suppressed VEGF-induced migration by 102% ± 4% ($P < 0.001$) and 72% ± 2% ($P = 0.002$), respectively (data not shown).

PEDF's Effect on VEGF-Induced Retinal Endothelial Cell Proliferation

VEGF is a retinal endothelial cell mitogen. To determine whether PEDF could suppress VEGF-induced growth, BRECs were exposed to 25 ng/mL VEGF for 4 days and DNA content evaluated. We have previously demonstrated that the total DNA content of a cell population is an accurate measure of cell number.[55] As demonstrated in Figure 6, 25 ng/mL VEGF increased DNA content 176% ± 11% ($P < 0.001$). Addition of 2 nM PEDF had no significant effect on basal cell growth. In contrast, 2 nM PEDF A and B suppressed VEGF-induced endothelial cell growth by 47.7% ($P < 0.001$) and 33.2% ($P = 0.009$), respectively. Addition of 20 nM PEDF had little additional effect, with inhibition of 48.8% and 41.4%, respectively ($P < 0.001$). Even at maximal PEDF-induced inhibition, VEGF-induced endothelial cell growth was still significantly higher than in control cells ($P = 0.001$).

DISCUSSION

The identification of PEDF in the vitreous and the demonstration of its inhibition of neovascularization in a corneal pocket assay[40,41] suggest a possible role for PEDF in regulating retinal neovascularization. To test this hypothesis, we used a highly reproducible mouse model of ischemia-induced retinal neovascularization.[52] In this study, intravitreous injection of either of two purified forms of recombinant PEDF resulted in marked inhibition of retinal neovascularization in all animals. These findings are consistent with a recent study that demonstrated that daily systemic injections of PEDF inhibit retinal neovascularization in mice with ischemic retinopathy.[42] In our study, the intravitreal mode of delivery of PEDF enabled the use of the contralateral eye as a control for each animal. In this setting, the consistent suppression of retinal neovascularization by PEDF across all animals offers independent confirmation of

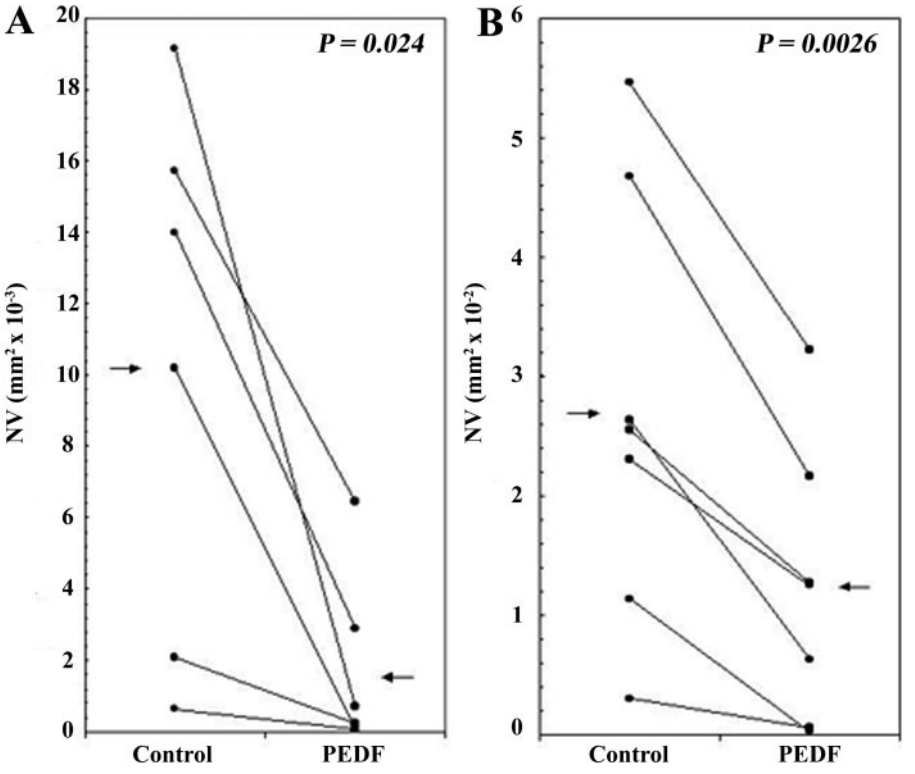

FIGURE 4. PEDF suppressed ischemia-induced retinal neovascularization in vivo (quantitative analysis). Results of injection of (**A**) PEDF A and (**B**) B are shown. Eyes from the same animal are connected by *solid lines. Arrows*: the mean of each group.

PEDF's inhibitory action on retinal neovascularization. In addition, the finding that PEDF given intravitreally is effective may have important clinical implications, because an intravitreal mode of treatment may help to minimize any possible side effects associated with systemic PEDF administration.

We have recently demonstrated that adenovirus (Ad)-based delivery of PEDF has an inhibitory effect in three mouse models of ocular neovascularization.[56] Although Ad-PEDF caused significantly more inhibition than empty Ad virus in each of the models, in the oxygen-induced ischemic retinopathy model the vector alone also caused substantial inhibition of neovascularization, compared with untreated eyes. This made it difficult to assess the impact of PEDF alone on retinal neovascularization. The present study demonstrates that the effect of PEDF alone (in the absence of additional factors related to viral infection or perhaps the immune response) is substantial. Injection of PEDF protein on postnatal days 12 and 14 was sufficient to reduce retinal neovascularization by 55% to 83%. This provides important evidence suggesting a potential role for local PEDF protein administration in the treatment of ischemic retinopathies (for instance, through strategies involving intravitreal injection or local sustained release of PEDF protein).

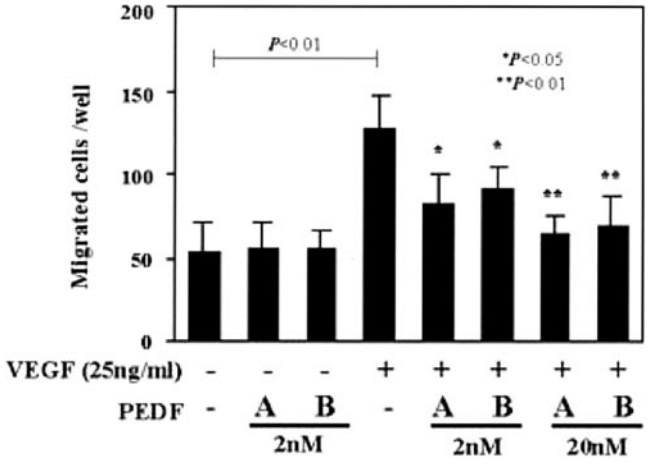

FIGURE 5. PEDF suppressed VEGF-induced retinal endothelial cell migration. BRECs were exposed to 25 ng/mL VEGF or vehicle and migration evaluated after 4 hours' exposure in the presence of PEDF at the concentrations indicated. Both the A and B species of isolated PEDF were evaluated. *Asterisks*: statistical analysis compared with VEGF-stimulated cells in the absence of PEDF (*fourth bar*). All data points were determined in triplicate and the experiment repeated twice, with similar results.

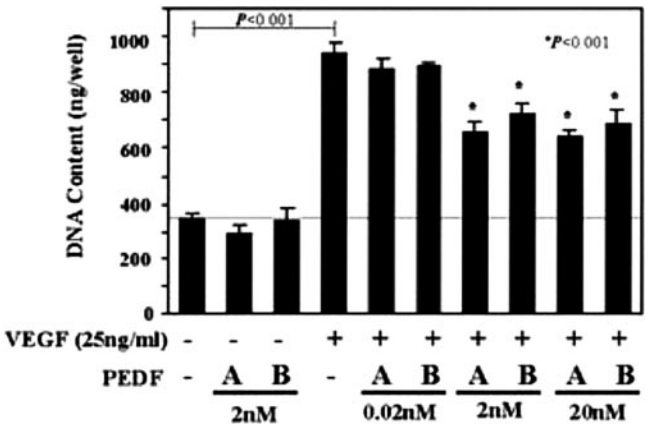

FIGURE 6. PEDF partially suppressed VEGF-induced retinal endothelial cell growth. BRECs were exposed to 25 ng/mL VEGF or vehicle for 4 days, after which DNA content was measured. Both the A and B species of isolated PEDF were evaluated. *Horizontal dotted line*: extent of basal cell growth. Results are expressed as the mean ± SD of triplicate determinations. *Asterisks*: statistical analysis compared with VEGF-stimulated cells in the absence of PEDF (*fourth bar*). The experiment was repeated twice, with similar results.

We obtained two forms of PEDF with similar molecular weight (denoted A and B) from our purification scheme. PEDF B appeared to comigrate with PEDF from human vitreous samples, as demonstrated in Figure 1D, suggesting that this may be the predominant form in the eye. It is noteworthy that both PEDF forms appeared to be bioactive in vivo and in vitro, and it is not clear whether there is a significant functional difference between these two forms. Results from endoglycosidase F digestion and LC-ESMS analysis of the intact proteins suggests that the differences observed by FPLC and SDS-PAGE between PEDF forms A and B are associated with glycosylation. Proof that PEDF A and B exhibit differences in glycopeptides containing NeuAc and HexNAc was derived from LC-ESMS analysis of tryptic peptides. The human PEDF precursor sequence contains one motif for N-linked glycosylation at Asn285 (Asn-X-Ser/Thr, where X is any amino acid except Pro) and also contains a total of 66 Thr and Ser residues where O-linked glycosylation may occur. The change in electrophoretic mobility of both PEDF A and B after endoglycosidase F digestion strongly suggests that both glycoforms contain N-linked oligosaccharide. The difference in electrophoretic mobility of PEDF A and B after endoglycosidase F digestion also suggests that the protein may contain additional O-linked oligosaccharide. Human recombinant PEDF appears to be processed differently in HEK293 cells than in infant hamster kidney cells where it exhibits a free N terminus, does not have the first 20 residues of the precursor sequence, and migrates as a single molecular species in SDS-PAGE.[46] It is notable that a single molecular species has also been reported for recombinant PEDF produced in HEK293 cells when engineered in the pCEP4 vector and expressed with a C-terminal histidine tag.[42] It is not clear why multiple forms of PEDF had not been observed previously in HEK293 cells. Proof of N-linked or O-linked glycosylation in native human PEDF and characterization of the N terminus of the recombinant protein expressed in HEK293 cells awaits further protein chemical analyses.

The mechanism of PEDF inhibition of retinal neovascularization in vivo is unknown. The role, if any, that PEDF glycosylation plays in the mechanism of inhibition remains to be determined. As mentioned earlier, VEGF has been demonstrated to play a major role in stimulating retinal neovascularization. We studied the effect of PEDF on VEGF-induced actions in microvascular endothelial cells that contribute to neovascularization, mitogenesis, and migration. VEGF has previously been shown to be mitogenic and motogeneic for endothelial cells[2,3]—in particular, for retinal endothelial cells.[6,57] Our in vitro data demonstrated an inhibitory effect of PEDF on VEGF-induced adrenal capillary endothelial cell migration, consistent with previous observations.[40] In addition, PEDF strongly inhibited VEGF-induced migration and proliferation of retinal endothelial cells. These results suggest that PEDF may regulate retinal neovascularization, at least in part, by suppressing the growth- and migration-promoting activities of VEGF. Better understanding of the biology and mechanism of action of PEDF may someday lead to the development of novel and more effective therapeutic approaches for the treatment of pathologic neovascular conditions.

Acknowledgments

The authors thank Pamela Barrows for technical assistance.

References

1. Aiello LP. Vascular endothelial growth factor: 20th-century mechanisms, 21st-century therapies. *Invest Ophthalmol Vis Sci*. 1997; 38:1647–1652.
2. Plate KH, Breier G, Weich HA, Risau W. Vascular endothelial growth factor is a potential tumour angiogenesis factor in human gliomas in vivo. *Nature.* 1992;359:845–848.
3. Ferrara N, Houck K, Jakeman L, Leung DW. Molecular and biological properties of the vascular endothelial growth factor family of proteins. *Endocr Rev.* 1992;13:18–32.
4. Shweiki D, Itin A, Soffer D, Keshet E. Vascular endothelial growth factor induced by hypoxia may mediate hypoxia-initiated angiogenesis. *Nature.* 1992;359:843–845.
5. Aiello LP, Northrup JM, Keyt BA, Takagi H, Iwamoto MA. Hypoxic regulation of vascular endothelial growth factor in retinal cells. *Arch Ophthalmol.* 1995;113:1538–1544.
6. Aiello LP, Avery RL, Arrigg PG, et al. Vascular endothelial growth factor in ocular fluid of patients with diabetic retinopathy and other retinal disorders. *N Engl J Med.* 1994;331:1480–1487.
7. Adamis AP, Miller JW, Bernal MT, et al. Increased vascular endothelial growth factor levels in the vitreous of eyes with proliferative diabetic retinopathy. *Am J Ophthalmol.* 1994;118:445–450.
8. Malecaze F, Clamens S, Simorre-Pinatel V, et al. Detection of vascular endothelial growth factor messenger RNA and vascular endothelial growth factor-like activity in proliferative diabetic retinopathy. *Arch Ophthalmol.* 1994;112:1476–1482.
9. Miller JW, Adamis AP, Shima DT, et al. Vascular endothelial growth factor/vascular permeability factor is temporally and spatially correlated with ocular angiogenesis in a primate model. *Am J Pathol.* 1994;145:574–584.
10. Pierce EA, Avery RL, Foley ED, Aiello LP, Smith LE. Vascular endothelial growth factor/vascular permeability factor expression in a mouse model of retinal neovascularization. *Proc Natl Acad Sci USA.* 1995;92:905–909.
11. Stone J, Chan-Ling T, Pe'er J, Itin A, Gnessin H, Keshet E. Roles of vascular endothelial growth factor and astrocyte degeneration in the genesis of retinopathy of prematurity. *Invest Ophthalmol Vis Sci.* 1996;37:290–299.
12. Aiello LP, Pierce EA, Foley ED, et al. Suppression of retinal neovascularization in vivo by inhibition of vascular endothelial growth factor (VEGF) using soluble VEGF-receptor chimeric proteins. *Proc Natl Acad Sci USA.* 1995;92:10457–10461.
13. Adamis AP, Shima DT, Tolentino MJ, et al. Inhibition of vascular endothelial growth factor prevents retinal ischemia-associated iris neovascularization in a nonhuman primate. *Arch Ophthalmol.* 1996;114:66–71.
14. Seo MS, Kwak N, Ozaki H, et al. Dramatic inhibition of retinal and choroidal neovascularization by oral administration of a kinase inhibitor. *Am J Pathol.* 1999;154:1743–1753.
15. Ozaki H, Seo MS, Ozaki K, et al. Blockade of vascular endothelial cell growth factor receptor signaling is sufficient to completely prevent retinal neovascularization. *Am J Pathol.* 2000;156:697–707.
16. Hanahan D, Folkman J. Patterns and emerging mechanisms of the angiogenic switch during tumorigenesis. *Cell.* 1996;86:353–364.
17. Smith LE, Shen W, Perruzzi C, et al. Regulation of vascular endothelial growth factor-dependent retinal neovascularization by insulin-like growth factor-1 receptor. *Nat Med.* 1999;5:1390–1395.
18. Smith LE, Kopchick JJ, Chen W, et al. Essential role of growth hormone in ischemia-induced retinal neovascularization. *Science.* 1997;276:1706–1709.
19. D'Amore PA. Mechanisms of retinal and choroidal neovascularization. *Invest Ophthalmol Vis Sci.* 1994;35:3974–3979.
20. Cai W, Rook SL, Jiang ZY, Takahara N, Aiello LP. Mechanisms of hepatocyte growth factor-induced retinal endothelial cell migration and growth. *Invest Ophthalmol Vis Sci.* 2000;41:1885–1893.
21. Antonelli-Orlidge A, Saunders KB, Smith SR, D'Amore PA. An activated form of transforming growth factor beta is produced by cocultures of endothelial cells and pericytes. *Proc Natl Acad Sci USA.* 1989;86:4544–4548.
22. O'Reilly MS, Holmgren L, Shing Y, et al. Angiostatin: a novel angiogenesis inhibitor that mediates the suppression of metastases by a Lewis lung carcinoma. *Cell.* 1994;79:315–328.
23. O'Reilly MS, Boehm T, Shing Y, et al. Endostatin: an endogenous inhibitor of angiogenesis and tumor growth. *Cell.* 1997;88:277–285.

24. O'Reilly MS, Pirie-Shepherd S, Lane WS, Folkman J. Antiangiogenic activity of the cleaved conformation of the serpin antithrombin. *Science.* 1999;285:1926–1928.
25. Good DJ, Polverini PJ, Rastinejad F, et al. A tumor suppressor-dependent inhibitor of angiogenesis is immunologically and functionally indistinguishable from a fragment of thrombospondin. *Proc Natl Acad Sci USA.* 1990;87:6624–6628.
26. Maione TE, Gray GS, Petro J, et al. Inhibition of angiogenesis by recombinant human platelet factor-4 and related peptides. *Science.* 1990;247:77–79.
27. Becerra SP, Sagasti A, Spinella P, Notario V. Pigment epithelium-derived factor behaves like a noninhibitory serpin: neurotrophic activity does not require the serpin reactive loop. *J Biol Chem.* 1995;270:25992–25999.
28. Becerra SP, Palmer I, Kumar A, et al. Overexpression of fetal human pigment epithelium-derived factor in *Escherichia coli*: a functionally active neurotrophic factor. *J Biol Chem*. 1993;268: 23148–23156.
29. Steele FR, Chader GJ, Johnson LV, Tombran-Tink J. Pigment epithelium-derived factor: neurotrophic activity and identification as a member of the serine protease inhibitor gene family. *Proc Natl Acad Sci USA.* 1993;90:1526–1530.
30. Tombran-Tink J, Chader GJ, Johnson LV. PEDF: a pigment epithelium-derived factor with potent neuronal differentiative activity. *Exp Eye Res.* 1991;53:411–414.
31. Taniwaki T, Becerra SP, Chader GJ, Schwartz JP. Pigment epithelium-derived factor is a survival factor for cerebellar granule cells in culture. *J Neurochem.* 1995;64:2509–2517.
32. Araki T, Taniwaki T, Becerra SP, Chader GJ, Schwartz JP. Pigment epithelium-derived factor (PEDF) differentially protects immature but not mature cerebellar granule cells against apoptotic cell death. *J Neurosci Res.* 1998;53:7–15.
33. DeCoster MA, Schabelman E, Tombran-Tink J, Bazan NG. Neuroprotection by pigment epithelial-derived factor against glutamate toxicity in developing primary hippocampal neurons. *J Neurosci Res.* 1999;56:604–610.
34. Bilak MM, Corse AM, Bilak SR, Lehar M, Tombran-Tink J, Kuncl RW. Pigment epithelium-derived factor (PEDF) protects motor neurons from chronic glutamate-mediated neurodegeneration. *J Neuropathol Exp Neurol.* 1999;58:719–728.
35. Cao W, Tombran-Tink J, Chen W, Mrazek D, Elias R, McGinnis JF. Pigment epithelium-derived factor protects cultured retinal neurons against hydrogen peroxide-induced cell death. *J Neurosci Res.* 1999;57:789–800.
36. Houenou LJ, D'Costa AP, Li L, et al. Pigment epithelium-derived factor promotes the survival and differentiation of developing spinal motor neurons. *J Comp Neurol.* 1999;412:506–514.
37. Cayouette M, Smith SB, Becerra SP, Gravel C. Pigment epithelium-derived factor delays the death of photoreceptors in mouse models of inherited retinal degenerations. *Neurobiol Dis.* 1999;6:523–532.
38. Jablonski MM, Tombran-Tink J, Mrazek DA, Iannaccone A. Pigment epithelium-derived factor supports normal development of photoreceptor neurons and opsin expression after retinal pigment epithelium removal. *J Neurosci.* 2000;20:7149–7157.
39. Cao W, Tombran-Tink J, Elias R, Sezate S, Mrazek D, McGinnis JF. In vivo protection of photoreceptors from light damage by pigment epithelium-derived factor. *Invest Ophthalmol Vis Sci.* 2001; 42:1646–1652.
40. Dawson DW, Volpert OV, Gillis P, et al. Pigment epithelium-derived factor: a potent inhibitor of angiogenesis. *Science.* 1999; 285:245–248.
41. Wu YQ, Becerra SP. Proteolytic activity directed toward pigment epithelium-derived factor in vitreous of bovine eyes: implications of proteolytic processing. *Invest Ophthalmol Vis Sci.* 1996;37: 1984–1993.
42. Stellmach V, Crawford SE, Zhou W, Bouck N. Prevention of ischemia-induced retinopathy by the natural ocular antiangiogenic agent pigment epithelium-derived factor. *Proc Natl Acad Sci USA.* 2001;98:2593–2597.
43. Duh E, Aiello LP. Vascular endothelial growth factor and diabetes: the agonist versus antagonist paradox. *Diabetes.* 1999;48:1899–1906.
44. Paborsky LR, Fendly BM, Fisher KL, et al. Mammalian cell transient expression of tissue factor for the production of antigen. *Protein Eng.* 1990;3:547–553.
45. Gorman C, Padmanabhan R, Howard BH. High efficiency DNA-mediated transformation of primate cells. *Science.* 1983;221:551–553.
46. Stratikos E, Alberdi E, Gettins PG, Becerra SP. Recombinant human pigment epithelium-derived factor (PEDF): characterization of PEDF overexpressed and secreted by eukaryotic cells. *Protein Sci.* 1996;5:2575–2582.
47. Laemmli UK. Cleavage of structural proteins during the assembly of the head of bacteriophage T4. *Nature.* 1970;227:680–685.
48. Crabb JW, West KA, Dodson WS, Hulmes JD, eds. *Amino Acid Analysis*. New York: John Wiley & Sons; 1997.
49. Crabb JW, Nie Z, Chen Y, et al. Cellular retinaldehyde-binding protein ligand interactions: Gln-210 and Lys-221 are in the retinoid binding pocket. *J Biol Chem.* 1998;273:20712–20720.
50. Kapron JT, Hilliard GM, Lakins JN, et al. Identification and characterization of glycosylation sites in human serum clusterin. *Protein Sci.* 1997;6:2120–2133.
51. West KA, Yan L, Miyagi M, et al. Proteome survey of proliferating and differentiating rat RPE-J cells. *Exp Eye Res*. 2001;73:479–491.
52. Smith LE, Wesolowski E, McLellan A, et al. Oxygen-induced retinopathy in the mouse. *Invest Ophthalmol Vis Sci.* 1994;35:101–111.
53. King GL, Goodman AD, Buzney S, Moses A, Kahn CR. Receptors and growth-promoting effects of insulin and insulinlike growth factors on cells from bovine retinal capillaries and aorta. *J Clin Invest.* 1985;75:1028–1036.
54. Klemke RL, Cai S, Giannini AL, Gallagher PJ, de Lanerolle P, Cheresh DA. Regulation of cell motility by mitogen-activated protein kinase. *J Cell Biol.* 1997;137:481–492.
55. Thieme H, Aiello LP, Takagi H, Ferrara N, King GL. Comparative analysis of vascular endothelial growth factor receptors on retinal and aortic vascular endothelial cells. *Diabetes.* 1995;44:98–103.
56. Mori K, Duh E, Gehlbach P, et al. Pigment epithelium-derived factor inhibits retinal and choroidal neovascularization. *J Cell Physiol.* 2001;188:253–263.
57. Simorre-Pinatel V, Guerrin M, Chollet P, et al. Vasculotropin-VEGF stimulates retinal capillary endothelial cells through an autocrine pathway. *Invest Ophthalmol Vis Sci.* 1994;35:3393–3400.